Distribution of charge on photoreceptor disc membranes and implications for charged lipid asymmetry

Francis C. Tsui, Steven A. Sundberg, and Wayne L. Hubbell
Jules Stein Eye Institute and Department of Chemistry and Biochemistry, University of California, Los Angeles, California 90024-1771

ABSTRACT A novel spin labeling technique is used to determine both the inner and outer surface potentials of isolated rod outer segment disc membranes and of reconstituted membranes containing rhodopsin with defined lipid compositions. It is shown that these potentials can be accounted for in a consistent manner by the accepted model of rhodopsin, the known lipid composition, and the Gouy-Chapman theory, provided the charged lipid is asymmetric in the membrane, with ~75% on the external surface.

INTRODUCTION

The disc membrane of the vertebrate photoreceptor rod outer segment (ROS)[1] has a particularly simple composition, as ~95% of the total membrane protein is the visual pigment rhodopsin. The lipid composition is known, and models have been proposed for the tertiary structure of rhodopsin based on a diverse body of physical and chemical information (for recent reviews see Hargrave, 1982; Chabre, 1985; Findlay, 1986*a* and *b*; Ovchinnikov, 1987). Furthermore, rhodopsin is now recognized as a member of a widespread, structurally homologous family of membrane receptors that function through the activation of a G-protein (Dohlman et al., 1987). As a result, this system is attractive for the investigation of molecular interactions in membranes and has served as a basis for the study of lipid-protein interactions (Watts et al., 1979; Deese et al., 1981; Baldwin and Hubbell, 1985; Ryba et al., 1987; Wiedmann et al., 1988) and receptor and G-protein interactions (Kuhn, 1984; Chabre, 1985; Chabre and Applebury, 1986; Schleicher and Hofmann, 1987).

Molecular interactions in membranes, as elsewhere, often involve an important electrostatic component. The interaction of charged lipids with proteins, protein–protein interactions, and interactions between membrane surfaces would all be expected to have significant electrostatic contributions. As a first step in analyzing the importance of electrostatic contributions to the above interactions, we have sought to determine the charge distribution at the disc membrane surfaces using experimentally determined surface potentials. Sundberg and Hubbell (1986) have recently developed a spin-label method for determining both the outer and inner surface potentials of phospholipid vesicles. In the present paper, this method is extended to the determination of the inner and outer surface potentials of the ROS disc membrane.

To use the measured surface potentials to obtain information about the actual charge distribution at the membrane surface, a theory relating the potential to the charge distribution and salt concentration must be available. The Gouy-Chapman theory has been shown to give an accurate account of charged surfaces of phospholipid bilayers by several independent experimental checks (McLaughlin, 1977, 1989). The theory assumes that all charge present is uniformly smeared over the surface and is located at the membrane solution interface. In general, this theory would not be expected to represent charged surfaces in membranes containing protein, because the charge is not uniformly smeared, and it is likely that protein charges will be distributed along a direction perpendicular to the membrane surface. Nevertheless, the Gouy-Chapman theory is frequently applied to native biological membranes without providing experimental or theoretical justification. In the present work, the degree to which the Gouy-Chapman theory accounts for the charged surfaces of membranes containing rhodopsin is examined. The approach taken is to compare experimentally determined surface potentials with those calculated from the Gouy-Chapman theory and an electrostatic model of the disc surface. The analysis presented properly accounts for the amphoteric nature of the surface (i.e., a pH-dependent charge density) and incorporates a consensus model of rhodopsin topology and the known lipid

Dr. Sundberg's present address is Cardiovascular Research Institute, University of California, San Francisco, CA 94143.

[1] *Abbreviations used in this paper:* DTAB, *N*-dodecyl-*N*,*N*,*N*-trimethylammonium bromide; DTT, dithiothreitol; EDTA, ethylenediaminetetraacetic acid; EPR, electron paramagnetic resonance; FFA, free fatty acid; Hepes, *N*-2-hydroxyethyl piperazine-*N*-2-ethanesulfonic acid; PC, phosphatidylcholine; PE, phosphatidylethanolamine; PS, phosphatidylserine; ROS, rod outer segment.

0006-3495/90/01/85/13 $2.00

composition. It is found that a self-consistent description is possible only with an asymmetric distribution of charged phospholipids.

In the following paper (Hubbell, 1989), a model is proposed which quantitatively accounts for an equilibrium asymmetry of charged lipids without invoking a direct interaction of lipid with protein.

Electrostatic model of disc membrane surface

We begin by discussing a simple electrostatic model for the surface of a membrane containing rhodopsin and a means for relating the predicted charge to a measurable surface potential. Fig. 1 shows a model for the orientation and polypeptide folding of bovine rhodopsin in the disc membrane based on other models in the literature (Ovchinnikov et al., 1982; Hargrave et al., 1983) but including the recently described fatty acyl thioesters on two adjacent cysteines (Ovchinnikov et al., 1988) and paying particular attention to the positioning of potentially charged residues. Whereas the relative positioning of the helices, their precise length, and the conformation of the loops and terminal domains are unknown, the general features, such as the net charge on the cytoplasmic and intradiscal surface, are probably reasonably well represented by this first-order model (see reviews by Chabre, 1985, 1989; Hargrave, 1982; Findlay, 1986*a* and *b*; Ovchinnikov, 1987 for discussions of these structural points). Of particular interest here are the residues that are charged in the region between pH 4 and 9. The bulk of such residues are located in the aqueous phases at the external and internal membrane faces. Exceptions are the protonated Schiff base at the attachment point of the retinal chromophore and two buried carboxyl groups. One of these groups is assumed to be the counter ion for the cationic Schiff base. There is no evidence regarding the ionization state of the other group. A priori, one would expect an isolated carboxyl in a low dielectric environment to be protonated, unless specifically stabilized. It is assumed that buried tyrosines, cysteines, and histidines have sufficiently shifted pK_as that they do not ionize unless involved in salt bridges.

Table 1 gives the distribution and intrinsic pK_as of the surface groups. The pK_as are average values for these side chains in proteins (Cantor and Schimmel, 1980). At neutral pH, rhodopsin is expected to be strongly bipolar, with the cytoplasmic surface positively charged and the intradiscal surface negatively charged. The membranes also contain the ionizable lipids PS and PE. The pK_a for the PS COOH group is 3.8, and the pK_as for the PS and PE amino groups are 9.8 and 9.6, respectively (Tsui et al., 1986).

The simplest electrostatic model for a membrane surface containing this protein is to assign each exposed group the charge it would have consistent with its pK_a and the surface pH, then compute a charge density at the membrane surface by assuming the total net charge to be smeared uniformly over the surface area occupied by the protein and its associated lipid. If charged lipids are present, their charge is simply added to that contributed by the protein. This assumes that the charges on the

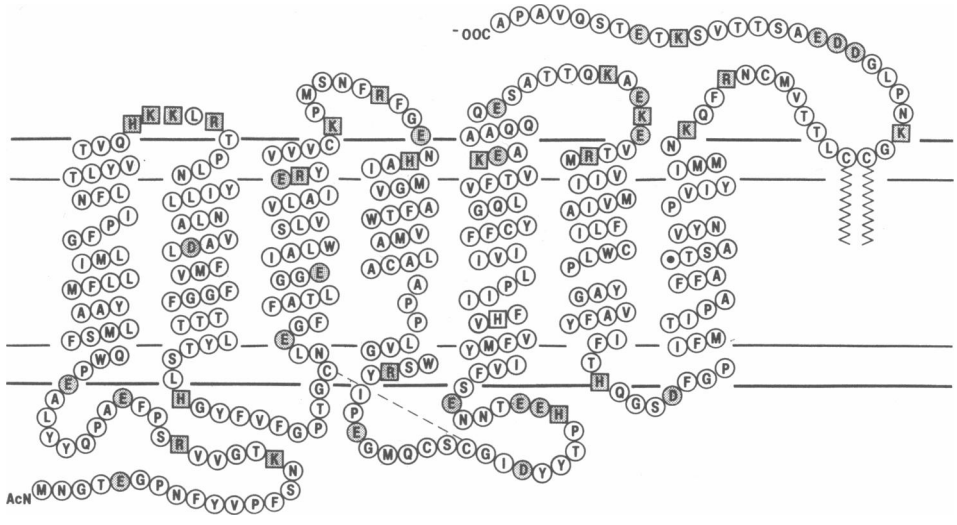

FIGURE 1 Organization of the rhodopsin polypeptide in the disc membrane. Potentially positively charged residues from arginine, lysine, and histidine are shown as shaded squares, and potentially negatively charged residues from carboxylates as shaded circles (except for the COOH terminal). The dashed line between cysteines 110 and 187 indicates the disulfide bond in rhodopsin (Karink et al., 1988). The dislocation in helices signify locations of proline residues. The circle with the dot (●) is lysine No. 296, the attachment site for retinal.

TABLE 1 Distribution and intrinsic pK_a values expected for surface amino acid side chains in rhodopsin

Group	No. on cytoplasmic surface*	No. on intradiscal surface*	pK_a‡
COOH-terminal	1	0	3.1
Asp + Glu	10	10	4.4
Tyr	2	9	9.6
Cys	2	1	8.0
Lys	9	1	10.2
Arg	5	2	12.0
His	2	3	7.0

*"Surface" groups are those located anywhere within the boundaries of polar headgroups outward toward the solution in Fig. 1.
‡From Cantor and Schimmel, 1980.

protein are located in the same plane as the lipid head group. The charge density computed in this way for an amphoteric surface depends on the surface pH. The surface pH is determined by the surface potential, which in turn is a function of the salt concentration. Accounting for these effects, the net charge density, in charges per square angstrom, can be expressed as

$$\sigma = \sum_i \frac{D_{bi}}{\frac{K_{bi}}{[H^+]}\exp\left(\frac{F\psi_0}{RT}\right) + 1} - \sum_j \frac{D_{aj}}{\left(\frac{[H^+]}{K_{aj}} + CK_{mj}\right)\exp\left(-\frac{F\psi_0}{RT}\right) + 1}, \quad (1)$$

where K_{bi} and K_{aj} are the dissociation constants for the basic and acidic residues of type i and j, respectively, D_{bi} and D_{aj} are the surface densities of the basic and acidic groups of type i and j (in groups per square angstrom), respectively, C is the concentration of monovalent cation in solution (in molarity), K_{mj} is the binding constant of the solution monovalent cation to the ionized acidic residue of type j, H^+ is the bulk hydrogen ion concentration (in molarity); ψ is the surface potential (volts), and the other symbols have their usual meaning. The sums extend over all ionizable groups, both protein and lipid. Binding of solution counter ions to surface negative charges has been included to allow for the weak binding of Na^+ and NH_4^+ to PS, with association constants of 0.7 and 0.2, respectively (Eisenberg et al., 1979; Tsui et al., 1986). To evaluate σ according to Eq. 1, the surface densities of each group must be determined. The surface density of a particular group of k, D_k, is calculated as

$$D_k = N_k/S_t = N_k/(S_r + N_L S_L), \quad (2)$$

where N_k is the number of groups of type k per rhodopsin at a particular surface (from protein or lipid), S_t is the total area occupied per rhodopsin on the membrane surface, S_r is the cross-sectional area of a single rhodopsin molecule, N_L is the number of lipids per rhodopsin at the surface of interest, and S_L is the surface area occupied per lipid. Methods for calculating the D_ks for different systems and values for the constants are presented in Materials and Methods.

Finally, the net charge density is related to the surface potential according to Gouy-Chapman theory:

$$\sigma = (C^{1/2}/136.6)\sinh(ZF\psi_0/2RT). \quad (3)$$

For a specific distribution of rhodopsin and lipid charges, both inner and outer surface potentials can be computed by simultaneous solution of Eqs. 1–3. The results of such calculations can be directly compared with experimental values for both surface potentials.

To provide a more critical comparison of the model with the experimental data, the salt dependence of surface potentials is explored for ROS disc vesicles and reconstituted membranes containing only neutral lipids. In the latter system the surface potentials are due entirely to the charges on the protein, and this measurement serves as a check on the electrostatic model of the protein. In addition, pH titrations of the disc membrane are compared to predictions of the model.

Although more sophisticated models for the relationship between charge density and surface potential are computationally tractable, a result of the present work is that the simplest model described above adequately represents the data within the experimental error and range of conditions studied. For comparison, we have also computed potentials for rhodopsin-containing membrane surfaces according to the discrete charge model of Nelson and McQuarrie (1975), and also according to a model in which the surface charge is allowed to distribute in various ways along a direction normal to the surface. The results of these calculations will be briefly discussed.

MATERIALS AND METHODS

Materials

Egg PC was purified according to the procedure of Singleton et al. (1965), and egg PS was purchased from Avanti Polar Lipids, Inc. (Birmingham, AL). The purity of the lipids was confirmed by thin-layer chromatography. Dark-adapted frozen bovine retinas were obtained from J. A. Lawson (Lincoln, NE) and were stored at −80°C before use. Hydroxylapatite (DNA grade) was purchased from Bio-Rad Laboratories (Richmond, CA), and DTAB was synthesized by the procedure of Hong and Hubbell (1973). The spin labeled amphiphile (I), *N,N*-dimethyl-*N*-nonyl-*N*-tempoyl ammonium bromide, was synthesized as described previously (Hubbell et al., 1970).

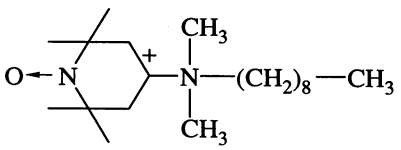

Scheme 1

Isolation of rod outer segment membranes

ROS disc membranes were isolated from 50 dark-adapted frozen bovine retinas according to the procedures described by Schnetkamp et al. (1979) under dim red light. All sucrose solutions were made with a buffer containing 20 mM Hepes, 1 mM $CaCl_2$, and 0.2 mM EDTA, pH 7.4. The ROS were collected from the uppermost dense band and washed once with 50 ml of 600 mM sucrose in buffer. ROS were resuspended in 600 mM sucrose, 5% Ficoll 400, 20 mM Hepes, and 4.4 mM Arginine, pH 6.8, to a final concentration of rhodopsin of ~150 μM for −30°C storage.

Preparation of reconstituted membranes

ROS isolated as described above were lysed by two washes with dilute buffer (1 mM Hepes, pH 6.8) and purification of rhodopsin was accomplished by chromatography on hydroxylapatite according to the procedure of Hong et al. (1982). To form the reconstituted membrane, 2–3 ml of a solution containing PC or PC and PS, 100 mM DTAB, 15 mM sodium phosphate, and 1 mM DTT at pH 6.8 was added to the purified rhodopsin in detergent to give a PC/rhodopsin molar ratio of ~100:1 or PC/PS/rhodopsin of ~95:5:1. Detergent was removed by dialysis under argon at 4°C against 5 mM Hepes, pH 6.8. Dialysis was continued for 4 d against an external volume of 1 liter of buffer and changed at least 10 times to ensure complete detergent removal. The concentration of rhodopsin was determined from the absorbance at 498 nm using a molar extinction coefficient of 42,000 (Hong and Hubbell, 1973). The phosphate assay of Bartlett (1959) was used to determine the final phospholipid content of the membranes.

Preparation of disc and reconstituted membrane vesicles for surface potential measurements

Aliquots of ROS stored as above in Hepes buffer with sucrose and Ficoll 400 were lysed and Ca^{++} depleted by two washes with 1 mm Hepes, 1 mm EDTA, and 0.5 μM of the Ca^{++} ionophore A23187, pH 7.2. The resulting pellet was resuspended in buffer with the desired pH value and either sonicated under argon for 15–30 s at 30 W in an ice bath for potentiometric titration (microtip sonicator, Heat Systems Ultrasonics, Inc., Danbury, CT) or allowed to equilibrate at room temperature in the desired medium. The average diameter of the sonicated vesicles was 600 ± 60 Å as determined by negative stain electron microscopy (Ojcius, 1985).

Reconstituted membranes obtained from the procedures described in a previous section were washed twice by centrifugation in 2 mM Hepes, 1 mM arginine, pH 7.3. The resulting pellet was resuspended in 1.5 ml of the same buffer containing the desired ionic composition and sonicated under argon for 60 s at 30 W in an ice bath. The average diameter of the vesicles was found to be ~600 Å by negative staining.

Determination of surface potentials from EPR spectra

The method used to determine the inner and outer surface potentials from the partitioning of spin label (I) was that developed by Sundberg and Hubbell (1986). The main points of the method are outlined below, but the original reference should be consulted for details. When (I) is mixed with membrane vesicles, it rapidly (within the mixing time of ~40 ms) comes to equilibrium with the external vesicle surface. In the presence of trace amounts of tetraphenylboron, which acts as a carrier, it slowly (~30 s) relaxes across the membrane and comes to a binding equilibrium with both the inner and outer surface. The mole number partition coefficient of (I) at any time during this process [$\lambda(t)$] is related to the amplitude of the high-field EPR resonance [$A(t)$] according to

$$\lambda(t) = [N_b(t)/N_f(t)] = [(A_f^\circ - A(t)]/[A(t) - (\beta/\alpha)A_f^\circ], \quad (4)$$

where N_b and N_f are the numbers of moles of (I) bound and free, respectively, A_f° is the spectral amplitude in the absence of membranes, and β/α is a constant with a value of −0.035 (Sundberg and Hubbell, 1986). Thus a measurement of the amplitude $A(t)$ allows the determination of $\lambda(t)$. From this relaxation experiment, two quantities are determined: $\lambda(0)$ from the amplitude immediately after mixing and $\lambda(\infty)$ from the amplitude at the final equilibrium. These quantities are related to the inner and outer surface potentials according to

$$\psi_o = -(RT/ZF) \ln [\lambda(0)/\lambda'(0)] \quad (5)$$

$$\psi_i = -\frac{RT}{ZF}\left\{\ln\left[\lambda(\infty) - \frac{\lambda(0)}{1 + (V_i/V_o)}\right] - \ln\left[\frac{K_i}{K_o}\frac{V_{mi}}{V_{mo}}\frac{\lambda'(0)}{1 + V_i/V_o}\right]\right\}, \quad (6)$$

where ψ_o and ψ_i are the outer and inner surface potentials, $\lambda'(0)$ is the $t = 0$ partition coefficient (to the outer surface) in the absence of a surface potential, V_i and V_o are the internal volume and external solution volume per vesicle, respectively, V_{mi} and V_{mo} are the volumes of the membrane phases on the inner and outer surfaces to which (I) partitions, and K_i and K_o are the equilibrium binding constants of (I) to the inner and outer surface.

To use these equations, the V_{mi}/V_{mo}, V_i/V_o, $\lambda'(o)$, and K_i/K_o must be determined. The ratio V_{mi}/V_{mo} is calculated directly from the size of the spherical vesicles as previously described (Cafiso and Hubbell, 1978). For reconstituted vesicles of 600 Å diameter,

$$V_i/V_o = A_{498}/(211 - 1.73\,A_{498}).$$

This equation is derived assuming a cross-sectional area of 1,000 Å^2 for a rhodopsin molecule, an average area per phospholipid of 70 Å^2, a membrane thickness of 50 Å, and an extinction coefficient for rhodopsin of 42,000 per cm at 498 nm. For ROS disc vesicles from osmotic lysis (diameter ≃ 5,000 Å), the inner and outer radii may be taken as equal, and it can be shown that

$$V_i/V_o = A_{498}/(21 - A_{498}).$$

This equation assumes a total area of 4,000 Å^2 per rhodopsin and its associated lipid at the membrane surface, and the same extinction coefficient given above. The above values for the molecular areas are discussed below.

To obtain $\lambda'(o)$, the binding is determined at $t = 0$ at the isoelectric point of the surface, where the net charge density and potential are zero. This is established by finding the pH at which the binding of (I) to the external surface is ionic strength independent. For reconstituted membranes containing rhodopsin and PC, the isoelectric point for the outer surface is at neutral pH, as will be shown below. Because the reconstituted membranes are compositionally symmetric, $K_i \simeq K_o$ (Cafiso and Hubbell, 1978). With these values, Eqs. 5 and 6 can be used to

determine ψ_o and ψ_i from the experimental values of $\lambda(0)$ and $\lambda(\infty)$ determined from a relaxation experiment.

For disc vesicles, it was found that both $\lambda(0)$ and $\lambda(\infty)$ are almost independent of ionic strength between pH 4.0 and 4.5. This implies that both ψ_o and ψ_i are very close to zero. Thus both the inner and outer surfaces appear to have similar isoelectric points, within experimental error. At pH ~4.3 and in the presence of 0.2 M salt to screen any residual potential, $\lambda'(0)$ was determined. Eq. 6 can then be used to find K_i/K_o from any set of relaxation data. With these values, Eqs. 5 and 6 can be used to find ψ_i and ψ_o at any other set of experimental conditions.

EPR measurements

Unless otherwise stated, all EPR measurements were carried out with a final spin label concentration of 25 μM and a rhodopsin concentration of 35–60 μM. At these concentrations, there were not more than 0.5 spin labels per rhodopsin, and typically 0.25 per rhodopsin. The model E-109 spectrometer (Varian Associates, Inc., Palo Alto, CA), interfaced to a model 1280 data acquisition system (Nicolet Instrument Corp., Madison, WI), was operated at X-band with a microwave power of 10 mW.

Rapid mixing experiments were carried out with a pneumatically driven plunger mechanism holding two syringes (Cafiso and Hubbell, 1982). One syringe contained spin label in appropriate buffer and ionic strength and the other contained the vesicle sample in the same buffer and ionic strength, with 1 μM gramicidin to prevent the buildup of transmembrane proton gradients, and 1 μM tetraphenylboron for enhancement of spin label transmembrane migration. The spectrometer was set to the high field line of the nitroxide spectrum and the amplitude of that peak was monitored as a function of time following the mixing of the spin label with the vesicle sample. This directly provides $\lambda(t)$ through Eq. 4.

Potentiometric titration of disc membrane vesicles

To complement the spin label binding studies, we also performed potentiometric titrations of disc membrane vesicles. All titrations were carried out under an argon atmosphere. Samples were prepared by diluting the stock membranes described in a previous section with 10, 50, or 100 mM NaCl to a final concentration of 0.25 mg/ml of rhodopsin in a total volume of 24 ml. Gramicidin, two to three molecules per vesicle, was added to prevent the build-up of transmembrane proton or sodium ion gradients. All experiments were carried out in plastic containers to prevent proton adsorption to the glass surface. The pH of the vesicle suspension was first adjusted to 4.3, near the isoelectric point, and then titrated with 20 mM NaOH. The titration curve of the membrane suspension, after subtraction of a blank titration curve, was used to deduce the number of protons released at different bulk pH values.

Calculation of surface densities for rhodopsin charged groups

The computation of surface densities for potentially charged groups on rhodopsin is different for reconstituted and ROS disc membranes due to different input information. For reconstituted membranes, the known quantities are the cross-sectional area of rhodopsin, the area occupied by a lipid molecule, and the membrane composition. In this case, the densities at each surface are calculated according to the second form of Eq. 2. The cross-sectional area of rhodopsin (S_r) lies in the range 800–1,200 Å^2 (Watts et al., 1979; Corless et al., 1982; Dratz et al., 1985) and S_r = 1,000 Å^2 will be used in the calculations. The total number of lipids per rhodopsin is determined by phosphate assay as described above. Egg yolk PC is the lipid used as the host for reconstitution in the present experiments. A value of S_L = 70 Å^2/molecule has consistently been found to be an appropriate choice in relating charge densities to surface potentials in systems containing this lipid as host (Castle and Hubbell, 1976; Sundberg and Hubbell, 1986). The same value is appropriate for egg PS in egg PC host bilayers up to at least 15 mol% (Tsui et al., 1986). For small vesicles in which the inner and outer surface areas are different, the number of lipids (N_L) at each surface is different and is calculated from the spherical vesicle geometry.

For ROS disc membranes, the number of lipids per rhodopsin varies from report to report, and the area per molecule for the disc lipids is unknown. However, the total surface area per rhodopsin is known to lie in the range of 3,500–4,500 Å^2 (Liebman et al., 1987; Amis et al., 1981; Krebs and Kuhn, 1977), and we will employ S_t = 4,000 Å^2 in the first form of Eq. 3 to compute group surface densities for osmotically lysed disc membrane vesicles.

RESULTS

Surface potentials of reconstituted membranes containing rhodopsin and phosphatidylcholine

Reconstituted membranes containing rhodopsin and PC are of interest here because the only net charge is due to rhodopsin itself. Thus, measured surface potentials reflect the charge distribution on the protein without contributions from the lipid. The reconstituted rhodopsin-PC vesicles used here are similar to those described by Fung and Hubbell (1978*a* and *b*), with an average diameter of ~600 Å as determined from negative stain and freeze-fracture electron microscopy (data not shown) and a mole ratio of lipid to rhodopsin of 110:1. Rhodopsin in the native disc membrane is completely oriented with the carboxy-terminal facing the external (cytoplasmic) surface. This orientation is referred to as "normal". As expected, the reconstituted vesicles do not reproduce this high degree of orientation. Fung and Hubbell showed that reconstituted vesicles of this size had an orientational distribution of rhodopsin of ~60:40, normal/inverted.

The inner and outer surface potentials measured by the spin label technique for the rhodopsin-PC reconstituted vesicles at pH 7.3 are shown as a function of salt concentration in Fig. 2 *a*. First, note the rather remarkable result that the outer surface potential is essentially zero and independent of ionic strength, even in the presence of a high concentration of a charged protein. Thus the outer membrane surface is isoelectric at pH 7.3. This can occur only if the net outer charge density at the membrane surface is zero. The inner surface potential is relatively small and negative.

Surface potentials for the reconstituted membranes can be predicted from the rhodopsin model with Eqs. 1–3

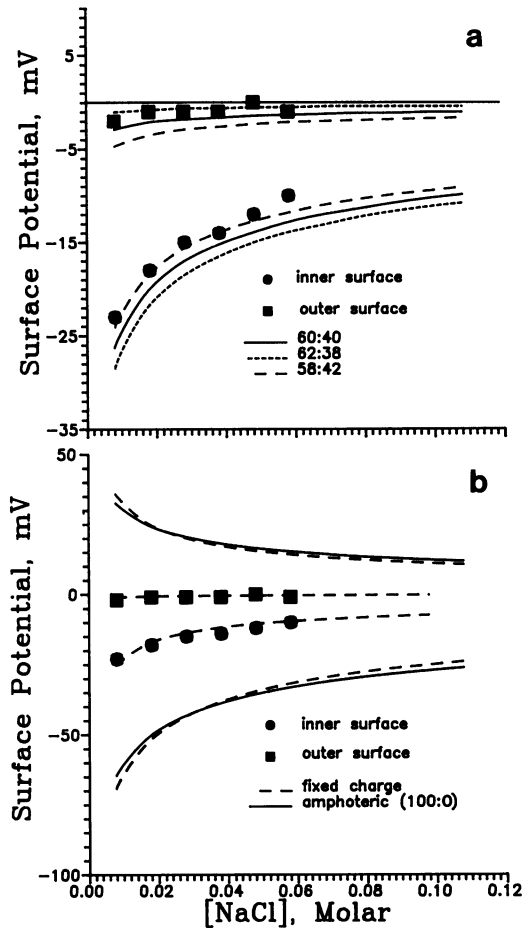

FIGURE 2 Surface potentials of reconstituted membranes containing PC and rhodopsin. (*a*) The points are experimental values for the outer and inner surface potentials estimated by the spin-label partition method at pH 7.3. Solid curves are calculated according to the model described in the text using a vesicle diameter of 600 Å, and 110 lipids per rhodopsin and a rhodopsin orientation of 60:40, normal to inverted. Dashed curves indicate the sensitivity of the calculation to different orientational distributions of rhodopsin. The standard error in the measured potential is about ±3 mV. (*b*) The points are the experimental values for the outer and inner surface potentials. Solid lines are computed according to the amphoteric model for the PC vesicles described in *a* but with 100:0 orientation of rhodopsin to illustrate the strongly bipolar nature of the protein. The dashed lines are the best fits to a fixed charge Gouy-Chapman model (see text).

as discussed above. The solid lines in Fig. 2 *a* show the predicted inner and outer surface potentials as a function of salt concentration for a rhodopsin orientational distribution of 60:40 and using the pKa values for the amino acid side chains given in Table 1. As can be seen, the fit to the experimental data is tolerable, although the calculated values are slightly more negative than the measured. Thus the model correctly predicts the isoelectric nature of the outer surface at neutral pH. The occurrence of near-zero net charge on the outer surface is a consequence of a close balance of positive charge from the normal rhodopsin orientation with negative charge from the inverted orientation. The sensitivity of the calculated result to the orientational distribution of rhodopsin is indicated by the dashed lines in Fig. 2 *a*, which correspond to orientational distributions of 58:42 and 62:38.

Fig. 2 *b* again shows the experimental data for the inner and outer surface potentials together with the calculated values of these potentials that would be expected if the rhodopsin were perfectly oriented (100:0) as in ROS disc membrane vesicles, but with no charged lipid (solid lines). The potentials are large in magnitude and of opposite sign, emphasizing the striking polarity of the rhodopsin molecule. This suggests that measurement of surface potential asymmetry will be a powerful means of assaying orientation in attempts at asymmetric reconstitution in the rhodopsin system.

To get a feeling for the importance of treating the surface as amphoteric (i.e., for including the variation of surface charge with salt concentration), values of the surface potentials computed from the amphoteric model for the 100:0 rhodopsin orientation were least-square fit to a fixed charge model. The results are shown as the dashed lines in Fig. 2 *b*. The best-fit fixed charge density is close to the average value of the charge density predicted by the amphoteric model, in which charge density varies with salt concentration. The deviations of the fixed charge model from the complete amphoteric model are most significant at low salt, where small changes in charge density produce large changes in potential. At high salt, variations in charge density are more effectively screened. This simple model is quite adequate for approximate work.

Surface potentials of reconstituted membranes containing PC and PS

To check the analysis and the amphoteric model, we prepared reconstituted membranes with known quantities of PS added. It was previously shown that the surface potentials of PC/PS vesicles, as measured by the spin label method, are accurately described by an amphoteric model (Tsui et al., 1986). Thus, known quantities of PS added to the PC-rhodopsin membranes should produce predictable changes in the surface potential as long as the presence of the protein does not interfere with the measurement. The vesicles were prepared from a mixture of PC/PS (95:5 mole ratio) with a total lipid/rhodopsin ratio of 110:1 in the final membranes. The average vesicle diameter was 600 Å, the same as for the reconstituted membranes with pure PC.

Fig. 3 shows experimentally determined surface poten-

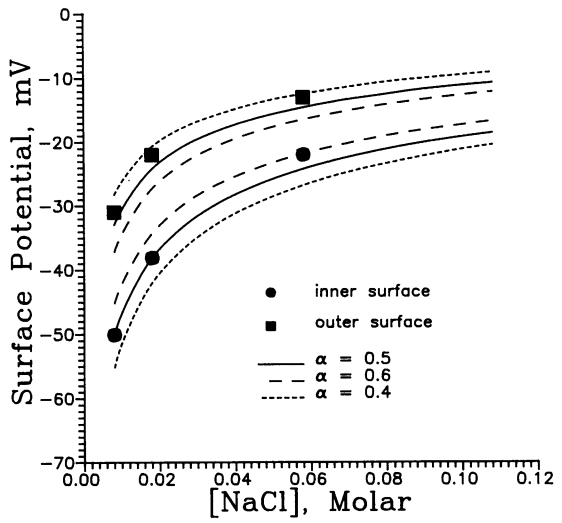

FIGURE 3 Surface potentials of reconstituted membranes containing PC + PS (95:5) and rhodopsin. The points are the experimental values for the outer and inner surface potentials at pH 7.3, as estimated by the spin label method. The solid curves are calculated according to the model described in the text using a vesicle diameter of 600 Å, 110 total lipids per rhodopsin, a rhodopsin orientation of 60:40, normal to inverted, and a symmetric distribution of PS ($\alpha = 0.5$). The dashed curves indicate the sensitivity of the result to different values of the PS asymmetry. The standard error in the experimental potential is about ±3 mV.

tials and the values calculated from the amphoteric model for a rhodopsin orientational distribution of 60:40 with a symmetrical distribution of PS. Care must be taken in describing what is meant by "asymmetry" of a lipid in vesicles of small radius where the outer and inner surface areas are unequal. In this case the fraction of a particular lipid on the outer surface will be >0.5 even for an unbiased distribution. This effect becomes important for spherical vesicles of outer radius less than ~1,000 Å. Lipid asymmetry is conveniently described by an "asymmetry" parameter, α, defined as

$$\alpha(\mathrm{k}) = D_{\mathrm{ok}}/(D_{\mathrm{ok}} + D_{\mathrm{ik}}), \quad (7)$$

where D_{ok} and D_{ik} are the surface densities of group k on the outer and inner surface, respectively. Alpha is unity for complete asymmetry with lipid k exclusively on the outer surface, 0.5 for an unbiased distribution, and 0 for asymmetry with k completely on the inner surface. The value of α is equal to the fraction of lipid k on the outer surface in an equivalent planar surface. The solid curves in Fig. 3 are for a PS distribution with $\alpha = 0.5$, a symmetric distribution.

As can be seen, the model accounts well for the perturbation induced by the addition of the PS. In Fig. 3, surface potentials calculated for $\alpha = 0.4$ and 0.6 are shown by the dashed curves and indicate the sensitivity of the surface potential to the lipid asymmetry.

Osmotically lysed disc membranes

The amphoteric Gouy-Chapman model accounts reasonably well for the surface of the reconstituted membranes, giving some confidence in the treatment. The ROS disc membrane containing an unknown distribution of charged lipids using the same model for the protein is now considered.

Disc membrane vesicles prepared by osmotic lysis, as described in Methods, have an average diameter of ~5,000 Å as determined by negative stain and freeze-fracture electron microscopy (data not shown). Similar sizes have been reported by light scattering techniques (Amis et al., 1981). Rhodopsin accounts for ~95% of all protein in these isolated membranes (Amis et al., 1981). The peripheral proteins of the cGMP system have been removed by low–ionic strength washes in the presence of EDTA. Unlike the reconstituted membranes discussed above, the rhodopsin is essentially completely oriented in the native disc membranes, with the carboxy-terminal surface facing outward (Hargrave and Fong, 1977; Fung and Hubbell, 1978*b*). In addition, the vesicles contain PS that is charged at neutral pH.

The isoelectric point for the outer surface of disc membrane vesicles prepared by osmotic lysis has been determined by electrophoretic mobility to be 4.3 (Kitano et al., 1983). The binding of label (I) to disc vesicles is found to be independent of ionic strength for both inner and outer surfaces between pH 4.0 and 4.5. This can only occur if both surface potentials are near zero, implying no net charge density. Thus the spin label result agrees with the electrophoretic mobility data regarding the isoelectric point of the outer surface and adds the new result that the inner surface has an isoelectric point in this same region. Electrophoretic mobility is dominated by the charge at the outer shear plane (McLaughlin, 1985), while the spin label measures the potential at the surface of the bilayer. The agreement of the two approaches as to the isoelectric point is consistent with a model in which the net charge on rhodopsin is restricted close to the membrane surface.

At the isoelectric point, the ratio of the intrinsic binding constants of (I) to the inner and outer surface can be determined as described in Materials and Methods. For disc vesicles at pH 4.3 and 0.2 M salt, $K_i/K_o = 0.7$. Because these are binding constants at zero surface potential, the difference is due only to structural features of the membrane, as for example, a difference in fluidity on the inner and outer bilayer leaflet.

Fig. 4 shows the outer and inner surface potentials of osmotically lysed disc membrane vesicles as a function of

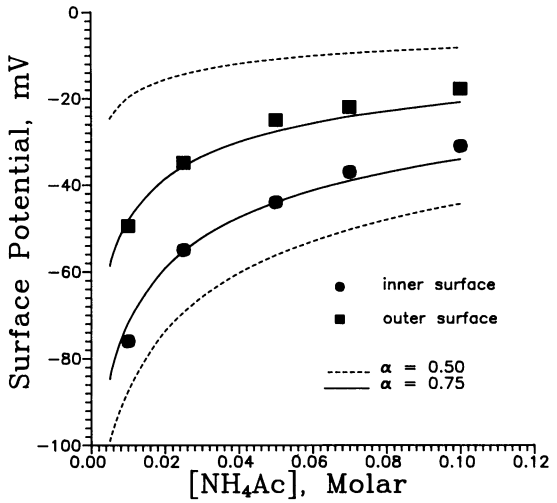

FIGURE 4 Surface potentials of osmotically lysed ROS disc membrane vesicles. The points are the experimental values of the surface potentials at pH 7.2 estimated by the spin label method. The solid curves are calculated according to the model described in the text with a rhodopsin orientation of 100:0, normal to inverted, 11 charged lipids per rhodopsin and 75% of the charged lipids on the external surface. Dashed line shows the calculated surface potentials with a symmetric distribution of charged lipid (α = 0.5). The standard error in the potential is about ±3 mV.

ammonium acetate concentration at pH 7.2 using the spin label method. The external surface potential is considerably more positive than the internal. Although membrane samples were usually analyzed within a few hours of preparation, surface potentials were reproducible after several days of storage at 4°C. Ammonium acetate was selected as an electrolyte because it is membrane permeable and shows normal screening behavior for a 1:1 symmetrical electrolyte (Sundberg and Hubbell, 1986).

Sufficient information exists to compute the expected surface potentials based on the amphoteric Gouy-Chapman model. From the known orientation of rhodopsin and the information in Table 1, the density of groups due to rhodopsin can be computed as discussed in Materials and Methods. The total charged phospholipid content is taken as 11 per rhodopsin (Miljanich et al., 1981). The solid lines in Fig. 4 show the surface potentials computed for ROS disc membranes according to the amphoteric model with an asymmetric charged lipid distribution of α = 0.75, i.e., where 75% of the charged lipid is on the external surface. The agreement with the experimental values of both inner and outer surface potentials is quite good. For comparison are shown curves calculated for a symmetric lipid distribution (α = 0.5; dashed lines). In the latter case, the outer potentials are far more positive and the inner potentials far more negative than the experimental values. With completely asymmetric distributions of charged lipids (α = 1.0), the deviations are about as great in magnitude but opposite in direction (not shown). The data can be accounted for only with an asymmetric charged lipid distribution with α in the neighborhood of 0.75. Including more than 12 charged lipids per rhodopsin leads to potentials too negative on both surfaces relative to the experimental values.

Titration of ROS disc vesicles

The isoelectric points are approximately equal for the outer and inner membrane surfaces for disc vesicles. Thus, the amount of base required to titrate the pH from the isoelectric point to a final pH is just equal to the total negative charge on the membrane surfaces. Unfortunately, the membranes are sufficiently permeable to protons and other ions that independent titration of the inner and outer surfaces cannot be carried out. The titration will simply give the total charge with no information on its distribution between the surfaces. Fig. 5 shows a titration curve for ROS disc membranes suspended in 50 mM NaCl plotted as protons dissociated per rhodopsin relative to the isoelectric point. In doing the titration, gramicidin was present to insure that the equilibrium pH inside and outside were the same. The number of protons dissociated per rhodopsin agrees reasonably well with that determined by Kitano et al. (1983) up to pH ~7.0, but at

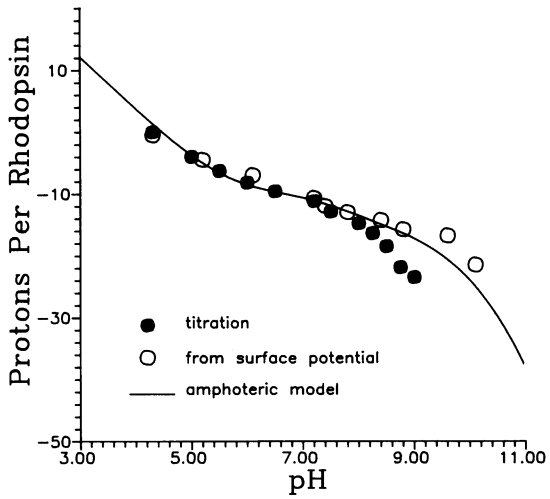

FIGURE 5 Titration curves for ROS disc membranes. Solid symbols are the number of protons dissociated from rhodopsin relative to the isoelectric point determined from direct pH titration of a suspension of membranes. Open circles are the number of protons dissociated relative to the isoelectric point calculated from experimental values of the surface potential as a function of pH. The solid curve is the titration curve calculated according to the model discussed in the text.

more basic pHs we find a greater number of protons dissociated. Also shown in the figure are the number of protons dissociated as estimated from surface potential measurements using spin label (I). The surface potentials determined for both surfaces as a function of pH were used to compute corresponding charge densities according to the Gouy-Chapman equation. The number of charges per rhodopsin determined in this way were then equated to the number of protons dissociated relative to the isoelectric point. The solid line in Fig. 5 is the titration curve calculated from Eqs. 1–3 using the pK_as given in Table 1 and a disc membrane composition containing (in addition to other neutral and zwitterionic lipids) 11 PS and 32 PE molecules per rhodopsin (Miljanich et al., 1981). In the range of pH from 4 to ~8.5, there is good agreement between the direct titration, the surface potential measurement, and the amphoteric model. In this range, the net charge on the membrane per rhodopsin changes from 0 to about −15. This is taken as further support of the amphoteric model of rhodopsin, and the ability of the Gouy-Chapman theory to relate the surface potential to the charge density in this complex system. Above a pH of 8.5, more protons are being removed from the surfaces than predicted by the amphoteric model. There are several possibilities for this discrepancy. For example, rhodopsin may be unfolding to some extent at basic pHs, exposing additional tyrosine side chains. Perhaps fatty acids with shifted pK_as could contribute protons in this region. This is a not an unreasonable possibility, because fatty acids in simple bilayers have pK_as near 7, about three units higher than the free caboxylate group (Von Tscharner and Radda, 1981). This is a result of the high solubility of the protonated form in the membrane interior. The large amount of protein in the ROS membrane would further increase the solubility of the protonated form (due to an increased intrabilayer dielectric constant) and lead to an even greater shift in pK_a, perhaps as high as 8.

More interesting is the fact that the surface potential, as measured by the spin label, indicates less charge density than expected from the proton dissociation in the basic pH range. Kitano et al. (1983) report a similar result in that the electrophoretic mobility of disc membrane vesicles remains nearly constant from pH 8 to 9.5, even though protons continue to be removed from the surfaces. Bangham and Papahadjopoulos (1966) have observed that the electrophoretic mobility of pure PS vesicles does not change between pH 5 and 12. McLaughlin has confirmed this result, and demonstrated that protons are in fact being removed from the vesicle surface in this pH range. Apparently, ion binding compensates for the charge generated by deprotonation of the PS amino group (McLaughlin, S., State University of New York Stony Brook, private communication).

DISCUSSION

The above results demonstrate that electrostatic potentials at a variety of membrane surfaces containing rhodopsin can be accounted for in a self-consistent way, employing the currently accepted model for rhodopsin structure, the known lipid composition of the membrane, and the Gouy-Chapman model of charged interfaces. Agreement between experimental and calculated potentials is found at both inner and outer surfaces over a range of salt concentrations, in the presence and absence of charged lipids, and with rhodopsin both oriented and unoriented in the ROS membrane. The only adjustable parameter in the calculation is the lipid asymmetry, and an asymmetry in charged lipid was required for agreement with the data only when rhodopsin was oriented in the ROS membrane. Predictions of the model are also in agreement with the pH dependence of the total surface charge as measured by titration and surface potential measurements in the range of pH 4–8. Other more complex models may also account for the data, but a conclusion of the above work is that the simple model described is sufficient.

Before commenting on the significance of the results, the application of the Gouy-Chapman model to a complex interface deserves some comment. Mathematically, the model gives an excellent description of the surface, but can its use in a relatively complex system be justified on physical grounds? Perhaps the most obvious potential weakness of the theory is that it assumes a uniform smeared charge, whereas real surfaces are composed of discrete charges. At charge densities where the surface intercharge spacing is short compared to the Debye length of the solution, the smeared charge model is justifiable. However it has been found experimentally that even for monovalent surface charge spacings at two to three times the Debye length, the model works well, and "discreteness of charge" effects have not been observed in the partitioning of charged amphiphiles like (I) (Winiski et al., 1986; Hartsel and Cafiso, 1986). The reasons for this are not entirely understood, but McLaughlin (1989) has reviewed the current ideas. Rhodopsin in the disc membrane is concentrated, about 25,000 copies/μm^2, and the average distance between rhodopsin surfaces is only ~25 Å. Under the least favorable conditions investigated (0.1 molar salt), this is 2.5 times the Debye length. Thus the smeared charge representation may be adequate within experimental error. This conclusion is examined in more detail below.

Rhodopsin has about +4 charges at neutral pH on the cytoplasmic surface of the disc membrane. Thus the charge distribution due to rhodopsin in a membrane is most correctly represented as clusters of four charges.

Nelson and McQuarrie (1975) have discussed quantitatively the electrostatics of discrete charge clusters on membrane surfaces, and in fact gave closed expressions for the electrostatic potential due to clusters of four charges on a square lattice. Thus the results of Nelson and McQuarrie can be used to represent the spatial distribution of potential at the disc outer surface in the discrete charge representation. Cafiso and Hubbell (1981) have shown that the "average" potential, Ψ, reported by spin label (I) in a spatially varying potential such as that from a discrete charge distribution is given by

$$\bar{\Psi} = \frac{RT}{ZF} \ln \sum_i \frac{A_i}{A} \exp\left[-\psi_i ZF/RT\right], \quad (8)$$

where ψ_i is the surface potential at the center of a small area element A_i at the membrane surface, A is the total surface area, and the other symbols have their usual meaning. The sum extends over the entire surface. Values of ψ_i can be obtained directly from the expressions of Nelson and McQuarrie. This offers an opportunity to compare the potential reported by the spin label (I) for the discrete charge distribution with that calculated from the smeared charge model.

The charge clusters considered by Nelson and McQuarrie and taken here to represent rhodopsin molecules in the disc membrane are shown in Fig. 6. The spacing between rhodopsin molecules is ~63 Å. The +4 charges on the molecule are located at a distance d relative to the center of the molecule and are at membrane-solution interface. For d = 12.7 Å, the charges are on the periphery of the molecule, as shown. For the purposes of approximate calculation, a 4,000 Å^2 area, representing one rhodopsin molecule and its associated lipids, was divided into a 160 × 25 Å^2 grid. For each 25 Å^2 element, the potential at the center was computed according to Nelson and McQuarrie and the discrete sum indicated in Eq. 8 was performed. The results of the calculation are shown in Table 2. The average potentials sensed by both positive ($\bar{\Psi}+$) and negative ($\bar{\Psi}-$) probe molecules have been calculated, because the difference between positive and negative probes is diagnostic for discrete charge effects (Winiski et al., 1986; Hartsel and Cafiso, 1986). As can be seen, the potentials are similar, and discrete charge effects are relatively small. The potentials reported by the positive and negative probes differ by at most 15% at high ionic strengths, and the smeared charge potential represents a fair approximation to either of them. These potentials in Table 2 do not include the contribution of the charged lipid, and cannot be compared to the experimental data.

If the charges on the protein are moved inward from the periphery, the average potential sensed by the probe will decrease. The furthest from the periphery that is reasonable to consider for the helical cluster protein is ~10 Å, the diameter of a helix. This corresponds to d = 6 Å. At this position, the potentials detected by a probe with the same sign as the protein are smaller by 20–40% over the range of salt concentrations from 0.01–0.1 M. Thus if all the net charge on the protein were clustered in the center of the protein, the spin label method would underestimate the charge when the potentials are interpreted in terms of the smeared charge model. In this particular situation, the charged lipid asymmetry would be overestimated. In this regard, it is significant that the asymmetry estimated on the basis of surface potentials agrees well with that determined by other means, as mentioned above.

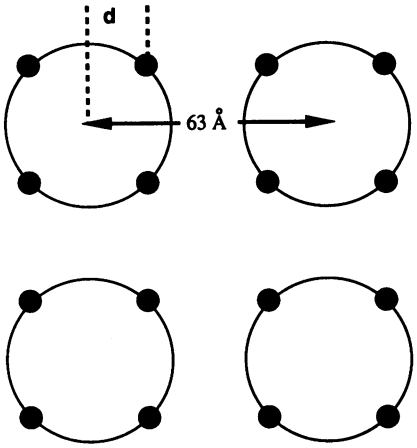

FIGURE 6 Discrete charge cluster representation for rhodopsin in the cytoplasmic surface of the disc membrane (based on the model of Nelson and McQuarrie, 1975). The rhodopsin molecules are located on a square lattice with a spacing of 63 Å, corresponding to an area per rhodopsin of 4,000 Å^2. The four charges on rhodopsin are located at the corners of a square with spacing d. In the figure, they are shown on the periphery of the molecule, corresponding to d = 12.7 Å for a rhodopsin diameter of 36 Å.

TABLE 2 Potentials sensed by positive ($\bar{\Psi}+$) and negative ($\bar{\Psi}-$) probes in a square lattice of charged proteins (Z = 4)

Concentration of monovalent salt	$\bar{\Psi}+$	$\bar{\Psi}-$	ψ_{sc}*
M	*mV*	*mV*	*mV*
0.01	56.6	62.9	56.0
0.02	40.2	46.1	42.9
0.05	24.2	28.7	28.9
0.08	18.5	21.7	23.3
0.10	16.3	18.8	20.9

*The smeared charge potential, i.e., the potential calculated by assuming the net charge to be uniformly smeared over the area of protein plus lipid.

An examination of most models of membrane proteins suggests that charged groups will be extended from the membrane surface. However, the Gouy-Chapman model with all the rhodopsin and lipid charge at the membrane solution interface accounts well for the data, leading to the suggestion that the rhodopsin net charge is not extended from the surface to an appreciable extent. To get a feeling for the effect of distributing charge perpendicular to the membrane surface, we computed potentials for various possibilities using the algorithm and program developed by Sharp and Brooks (1985). The models for the folding of the rhodopsin polypeptide proposed by various authors (Ovchinikov, 1982; Findlay, 1986*a* and *b*; Hargrave et al., 1983) and that in Fig. 1 suggest that a large fraction of the rhodopsin net charge on the outer surface is constrained to remain close to the interface to gain the maximum hydrophobic energy of burying the nonpolar helical segments.

From an examination of the model in Fig. 1, one finds approximately +6 net charges constrained to remain near the outer surface and −2 net charges possibly free to distribute according to whatever structure the loops may adopt. These are subjective estimates but provide the basis for an illustrative calculation. In the calculation, the charges from both the protein and lipid will be included. Fig. 7 shows the electrostatic potentials for the outer surface as a function of salt concentration for models in which the −2 net charge is distributed uniformly over layers 0, 10, and 20 Å thick, with the remainder of the charge (including that from the charged lipids) restricted to the surface. Also shown is the experimental data for the outer surface potential. It is clear that the model with the charge all at the surface fits the data best. However, a distribution with −2 charges over a layer 10–20 Å thick gives potentials that are only a few millivolts different over the entire range and is not experimentally distinguishable from all charges at the surface.

On the intradiscal surface, there are about −2 charges structurally constrained to the interface and perhaps −3 charges free to adopt extended structures. Fig. 7 also includes a model of the inner surface where −3 charges are allowed to distribute throughout shells of 0, 10, and 20 Å thickness with the remainder of the charge at the surface. Again, the model with the charge at the surface fits best. Distributions of −3 charges in a layer of 10 Å gives potentials ~5 mV less than the best fit. This is larger than the experimental error of about ±3 mV.

These are highly simplified models, but serve to indicate limitations in the conclusions drawn from the surface potential data. It is concluded that the net charge on rhodopsin is confined relatively close to the membrane surface, although the distribution of a net charge or two over a layer 10–20 Å thick could be accommodated by the data.

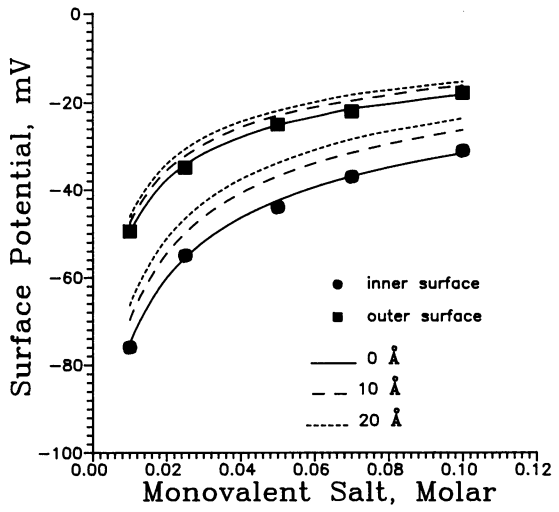

FIGURE 7 Predicted surface potentials for rhodopsin charges distributed perpendicular to the membrane surface. The inner and outer potentials for the ROS disc membrane are predicted according to a fixed charge Gouy-Chapman model for the following models: (*a*) all of the rhodopsin charge located at the membrane surfaces (*solid lines*); (*b*) −2 rhodopsin charge distributed over a 10- or 20-Å shell at the outer surface (*dashed lines, upper part of figure*); (*c*) −3 rhodopsin charges distributed over a 10- or 20-Å shell for the inner surface (*dashed lines, lower part of figure*). Also shown are the experimentally determined inner and outer potentials determined by the spin label method (*solid symbols*). See text for explanation of models. Standard error in the measured potentials is about ±3 mV.

The above conclusion is supported by other experimental data. Freeze-etching studies of ROS disc membranes reveal no protrusions within the 20-Å resolution of the replica (Chen and Hubbell, 1973). The intradiscal spacing in the native ROS is only 20 ± 5 Å (Korenbrot et al., 1973; Chabre and Cavaggioni, 1975). This limits the extent of protrusion of rhodopsin from this surface to ~10 Å or so. Support for the surface location of the rhodopsin charge also comes from measurements of its dipole moment. Petersen and Cone (1975) found the dipole moment of rhodopsin in solutions of Triton X-100 to be 720 D at the isoelectric point of the protein (5.3). The model of rhodopsin in Fig. 1 and the pK_as in Table 1 predict that at the isoelectric point for the whole rhodopsin molecule each surface of rhodopsin will have charges of magnitude 3.5 (and opposite in sign). To give a molecular dipole moment of 720 D, these charges would have to be separated by 46 Å, close to the membrane thickness.

Having justified the use of the Gouy-Chapman model to some extent, the data can be interpreted to support the proposed topology of rhodopsin with the net charge concentrated near the membrane surface and the existence of a pronounced lipid asymmetry with ~75% of the

PS on the external surface. This latter conclusion is of some interest, since there is not complete agreement in the literature as to the degree of lipid asymmetry in the ROS disc membrane. Drenthe et al. (1980*a* and *b*) found no lipid asymmetry in disc membranes using a combination of chemical labeling and phospholipase methods. Crain et al. (1978), using chemical labeling, reported that only 25–31% of the disc membrane PS was in the outer monolayer. Smith et al. (1977) reported that all the PS in the disc was in the outer monolayer. The result presented here, based entirely on electrostatic considerations, agrees most closely with that of Miljanich et al. (1981), who found 77–88% of the PS on the outer surface using chemical methods. A companion paper (Hubbell, 1989) offers a model which accounts for the origin of the asymmetry.

The above results provide a working electrostatic model of the disc membrane surface which can now be used as a basis for the investigation of electrostatic phenomena in this system. For example, the binding of metal ions, protons, and other charged species (including proteins) to either membrane surface could be readily investigated by the methods described here. It should also be possible to follow rhodopsin phosphorylation kinetics and stoichiometry in real time. Finally, surface potential measurements could serve as a valuable assay in reconstitution where asymmetric insertion of membrane protein is sought.

We would like to thank Drs. J. Trudell, P. Todd, and S. McLaughlin for many helpful discussions and careful readings of the manuscript.

This work was supported by National Institutes of Health grants 05216 to W. L. Hubbell, Postdoctoral Training grant EY-07026 to F. C. Tsui, Vision Research Center grant EY-00331 to the Jules Stein Eye Institute, and the Jules Stein Professor Endowment to W. L. Hubbell.

Received for publication 6 June 1989 and in final form 28 August 1989.

REFERENCES

Amis, E. J., D. A. Davenport, and H. Yu. 1981. Photopigment content of isolated bovine disk membrane vesicles. *Anal. Biochem.* 114:85–91.

Baldwin, P. A., and W. L. Hubbell. 1985. Effects of lipid environment on the light-induced conformational changes of rhodopsin. 2. Roles of lipid chain length, unsaturation, and phase state. *Biochemistry.* 24:2633–2639.

Bangham, A., and D. Papahadjopoulos. 1966. Biophysical properties of phospholipids. I. Interaction of phosphatidylserine monolayers with metal. *Biochim. Biophys. Acta.* 126:181–184.

Bartlett, G. R. 1959. Phosphorus assay in column chromatography. *J. Biol. Chem.* 234:466–468.

Cafiso, D. S., and W. L. Hubbell. 1978. Estimation of transmembrane potentials from phase equilibria of hydrophobic paramagnetic ions. *Biochemistry.* 17:187–195.

Cafiso, D. S., and W. L. Hubbell. 1981. EPR determination of membrane potentials. *Annu. Rev. Biophys. Bioeng.* 10:217–244.

Cafiso, D. S., and W. L. Hubbell. 1982. Transmembrane electric current of spin-labeled hydrophobic ions. *Biophys. J.* 39:263–272.

Cantor, C., and P. Schimmel. 1980. Biophysical Chemistry. Part I. The Conformation of Biological Membranes. Freeman Publications, San Francisco. 341 pp.

Castle, J. D., and W. L. Hubbell. 1976. Estimation of membrane surface potential and charge density from the phase equilibrium of a paramagnetic amphiphile. *Biochemistry.* 15:4818–4831.

Chabre, M. 1985. Trigger and amplification mechanisms in visual transduction. *Annu. Rev. Biophys. Biophys. Chem.* 14:331–360.

Chabre, M. 1989. Molecular mechanism of visual transduction. *Eur. J. Biochem.* 179:255–266.

Chabre, M., and M. Applebury. 1986. Interaction of photoactived rhodopsin with photoreceptor proteins: the cGmp cascade. *In* Molecular Mechanism of Phototransduction. H. Stieve, editor. Springer-Verlag, Berlin. 51–66.

Chabre, M., and A. Cavaggioni. 1975. X-Ray diffraction studies of retinal rods. II. Light effect on the osmotic properties. *Biochim. Biophys. Acta.* 382:336–343.

Chen, Y. A., and W. Hubbell. 1973. Temperature- and light-dependent structural changes in rhodopsin-lipid membranes. *Exp. Eye Res.* 17:517–532.

Coreless, J. M., D. R. McCaslin, and B. L. Scott. 1982. Two-dimensional rhodopsin crystals from disc membranes of retinal rod outer segments. *Proc. Natl. Acad. Sci. USA.* 79:1116–1120.

Crain, R. C., G. V. Marinetti, and D. F. O'Brien. 1978. Topology of amino phospholipids in bovine retinal rod outer segment disk membranes. *Biochemistry.* 17:4186–4192.

Deese, A. J., E. A. Dratz, F. W. Dahlquist, and M. R. Paddy. 1981. Interaction of rhodopsin with two unsaturated phosphatidylcholines: a deuterium nuclear magnetic resonance study. *Biochemistry.* 20:6420–6427.

Dohlman, H. G., M. G. Caron, and R. J. Lefkowitz. 1987. A family of receptors coupled to guanine nucleotide regulatory proteins. *Biochemistry.* 26:2657–2664.

Dratz, E. A., J. F. L. Van Breemen, K. M. P. Kamps, W. Keegstra, and E. F. J. Van Bruggen. 1985. Two-dimensional crystallization of bovine rhodopsin. *Biochim. Biophys. Acta.* 832:337–342.

Drenthe, E. H. S., S. L. Bonting, and F. J. M. Daemen. 1980*a*. Transbilayer distribution of phospholipids in photoreceptor membrane studied with various lipases. *Biochim. Biophys. Acta.* 603:117–129.

Drenthe, E. H. S., A. A. Klompmaker, S. L. Bonting, and F. J. M. Daemen. 1980*b*. Transbilayer distribution of phospholipids in photoreceptor membrane studied with trinitrobenzenesulfonate alone and in combination with phospholipase D. *Biochim. Biophys. Acta.* 603:130–141.

Eisenberg, M., T. Gresalfi, T. Riccio, and S. McLaughlin. 1979. Adsorption of monovalent cations to bilayer membranes containing negative phospholipids. *Biochemistry.* 18:5213–5223.

Findlay, J. B. C. 1986*a*. The structure of rhodopsin. *Photobiochem. Photobiophys.* 13:213–228.

Findlay, J. B. C. 1986*b*. The biosynthetic, functional, and evolutionary implications of the structure of rhodopsin. *In* Molecular Mechanism of Phototransduction. H. Stieve, editor. Springer-Verlag, Berlin. 11–30.

Fung, B. K.-K., and W. L. Hubbell. 1978*a*. Organization of rhodopsin in photoreceptor membranes. 1. Proteolysis of bovine rhodopsin in native

membranes and the distribution of sulfhydryl groups in the fragments. *Biochemistry.* 17:4396–4402.

Fung, B. K.-K., and W. L. Hubbell. 1978*b*. Organization of rhodopsin in photoreceptor membranes. 2. Transmembrane organization of bovine rhodopsin: evidence from proteolysis and lactoperoxidase-catalyzed iodination of native and reconstituted membranes. *Biochemistry.* 17:4403–4410.

Hargrave, P. A. 1982. Rhodopsin chemistry, structure and topography. *Prog. Retinal Res.* 1:1–50.

Hargrave, P. A., and S.-L. Fong. 1977. The amino- and carboxyl-terminal sequence of bovine rhodopsin. *J. Supramol. Struct.* 6:559–570.

Hargrave, P. A., J. H. McDowell, D. R. Curtis, J. K. Wang, E. Juszczak, S.-L. Hong, J. K. Mohanna Rao, and P. Argos. 1983. The structure of bovine rhodopsin. *Biophys. Struct. Mech.* 9:235–244.

Hartsel, S. C., and D. S. Cafiso. 1986. A test of discreteness-of-charge effects in phospholipid vesicles: measurements using paramagnetic amphiphiles. *Biochemistry.* 25:8214–8219.

Hong, K., and W. Hubbell. 1973. Lipid requirements for rhodopsin regenerability. *Biochemistry.* 12:4517–4523.

Hong, K., P. J. Knudsen, and W. L. Hubbell. 1982. Purification of rhodopsin on hydroxyapatite columns, detergent exchange, and recombination with phospholipids. *Methods Enzymol.* 81:145–150.

Hubbell, W. L. 1989. A transbilayer coupling mechanism for the formation of lipid asymmetry in biological membranes. Application to the photoreceptor disc membrane. *Biophys. J.* 57:99–108.

Hubbell, W. L., J. C. Metcalfe, S. M. Metcalfe, and H. M. McConnell. 1970. The interaction of small molecules with spin-labelled erythrocyte membranes. *Biochim. Biophys. Acta.* 219:415–427.

Karink, S. S., T. P. Sakmr, H.-B. Chen, and H. G. Khorana. 1988. Cysteine residues 110 and 187 are essential for the formation of correct structure in bovine rhodopsin. *Proc. Natl. Acad. Sci. USA.* 85:8459–8463.

Kitano, T., T. Chang, G. B. Caflisch, D. B. Piatt, and H. Yu. 1983. Surface charges and calcium ion binding of disc membrane vesicles. *Biochemistry.* 20:5500–5510.

Korenbrot, J. I., D. T. Brown, and R. A. Cone. 1973. Membrane characteristics and osmotic behavior of isolated rod outer segments. *J. Cell Biol.* 36:389–398.

Krebs, W., and H. Kuhn. 1977. Structure of isolated bovine rod outer segment membranes. *Exp. Eye Res.* 25:511–526.

Kuhn, H. 1984. Interaction between photoexcited rhodopsin and light activated enzymes in rods. *Prog. Retinal Res.* 3:123–156.

Liebman, P. A., K. R. Parker, and E. A. Dratz. 1987. The molecular mechanism of visual excitation and its relation to the structure and composition of the rod outer segment. *Annu. Rev. Physiol.* 49:765–791.

McLaughlin, S. 1977. Electrostatic potentials at membrane-solution interfaces. *Curr. Top. Memb. Transp.* 9:71–14.

McLaughlin, S. 1985. New experimental models for the electrokinetic properties of biological membranes: the location of fixed charges affects the electrophoretic mobility of model membranes. *Stud. Biophys.* 100:25–28.

McLaughlin, S. 1989. The electrostatic properties of membranes. *Annu. Rev. Biophys. Biophys. Chem.* 18:113–136.

Miljanich, G. P., P. P. Nemes, D. L. White, and E. A. Dratz. 1981. The asymmetric transmembrane distribution of phosphatidylethanolamine, phosphatidylserine, and fatty acids of the bovine retinal rod outer segment disc membrane. *J. Membr. Biol.* 60:249–255.

Nelson, A. P., and D. A. McQuarrie. 1975. The effect of discrete charges on the electrical properties of a membrane. *Int. J. Theor. Biol.* 55:13–27.

Ojcius, D. M. 1985. Ionic conductance of photoreceptor membranes and phospholipid vesicles measured with a phosphonium spin-label. Ph.D. thesis. University of California, Berkeley.

Ovchinnikov, Y. A. 1987. Probing the folding of membrane proteins. *Trends Biochem. Sci.* 12:434–438.

Ovchinnikov, Y. A., N. G. Abdulaev, M. Y. Feigina, I. D. Artomonov, A. S. Zolotarev, A. I. Moroshnikov, V. I. Martynow, M. B. Kostina, A. B. Kudelin, and A. S. Bogachuk. 1982. The complete amino acid sequence of visual rhodopsin. *Bioorg. Khim.* 8:1424–1427.

Ochinnikov, Y. A., N. G. Abdulaev, and A. S. Bogachuk. 1988. Two adjacent cysteine residues in the C-terminal cytoplasmic fragment of bovine rhodopsin are palmitylated. *FEBS (Fed. Eur. Biochem. Soc.) Lett.* 230:1–5.

Petersen, D. C., and R. A. Cone. 1975. The electric dipole moment of rhodopsin solubilized by Triton X-100. *Biophys. J.* 15:1181–1200.

Ryba, N. J. P., L. I. Horvath, A. Watts, and D. Marsh. 1987. Molecular exchange at the lipid-rhodopsin interface: spin-label electron spin resonance studies of rhodopsin-dimyristoylphosphatidylcholine recombinants. *Biochemistry.* 26:3234–3240.

Schleicher, A., and K. P. Hoffman. 1987. Kinetic study on the equilibrium between membrane-bound and free photoreceptor G-protein. *J. Membr. Biol.* 95:271–281.

Schnetkamp, P. P. M., A. A. Klompmakers, and F. J. M. Daemen. 1979. The isolation of stable cattle rod outer segments with an intact plasma membrane. *Biochim. Biophys. Acta.* 552:379–389.

Sharp, K., and D. Brooks. 1985. Calculation of the electrophoretic mobility of a particle bearing bound polyelectrolyte using the nonlinear Poisson-Boltzmann equation. *Biophys. J.* 47:563–566.

Singleton, W. S., M. S. Gray, M. L. Brown, and J. L. White. 1965. Chromatographic homogeneous lecithin purified from egg phospholipids. *J. Am. Oil Chem. Soc.* 42:53–56.

Smith, H. G., R. S. Fager, and B. J. Litman. 1977. Light-activated calcium release from sonicated bovine retinal rod outer segment discs. *Biochemistry.* 16:1399–1405.

Sundberg, S., and W. Hubbell. 1986. Investigation of surface potential asymmetry in phospholipid vesicles by a spin label relaxation method. *Biophys. J.* 49:553–562.

Tsui, F. C., D. M. Ojcius, and W. L. Hubbell. 1986. The intrinsic pKa values for phosphatidylserine and phosphatidylethanolamine in phosphatidylcholine host bilayers. *Biophys. J.* 49:459–468.

Von Tscharner, V., and G. K. Rada. 1981. Effect of fatty acids on the surface potential of phospholipid vesicles measured by condensed phase radioluminescence. *Biochim. Biophys. Acta.* 643:435–448.

Watts, A., I. Volotovski, and D. Marsh. 1979. Rhodopsin-lipid associations in bovine rod outer segment membranes. Identification of immobilized lipid by spin-labels. *Biochemistry.* 18:5006–5013.

Wiedmann, T. S., R. D. Pates, J. M. Beach, A. Salmon, and M. F. Brown. 1988. Lipid-protein interactions mediate the photochemical function of rhodopsin. *Biochemistry.* 27:6469–6474.

Winiski, A. P., A. C. McLaughlin, R. V. McDaniel, M. Eisenberg, and S. McLaughlin. 1986. An experimental test of the discreteness-of-charge effect in positive and negative lipid bilayers. *Biochemistry.* 25:8206–8213.